Proc. Natl. Acad. Sci. USA
Vol. 91, pp. 2517–2521, March 1994
Biochemistry

Three-dimensional structure of rat liver 3α-hydroxysteroid/dihydrodiol dehydrogenase: A member of the aldo-keto reductase superfamily

(x-ray crystallography/mammalian steroid-metabolizing enzyme/triose-phosphate isomerase barrel/steroid hormone, prostaglandin, and polycyclic aromatic hydrocarbon recognition/nonsteroidal antiinflammatory drugs)

SUSAN S. HOOG*, JOHN E. PAWLOWSKI†, PEDRO M. ALZARI‡, TREVOR M. PENNING†, AND MITCHELL LEWIS*§

*The Johnson Research Foundation, Department of Biochemistry and Biophysics and †Department of Pharmacology, University of Pennsylvania School of Medicine, Philadelphia, PA 19104-6084; and Unité d' Immunologie Structurale, Institut Pasteur, 25 rue du Dr. Roux, 75724 Paris cedex 15, France

Communicated by Paul Talalay, November 30, 1993 (received for review August 23, 1993)

ABSTRACT **The 3.0-Å-resolution x-ray structure of rat liver 3α-hydroxysteroid dehydrogenase/dihydrodiol dehydrogenase (3α-HSD, EC 1.1.1.50) was determined by molecular replacement using human placental aldose reductase as the search model. The protein folds into an α/β or triose-phosphate isomerase barrel and lacks a canonical Rossmann fold for binding pyridine nucleotide. The structure contains a concentration of hydrophobic amino acids that lie in a cavity near the top of the barrel and that are presumed to be involved in binding hydrophobic substrates (steroids, prostaglandins, and polycyclic aromatic hydrocarbons) and inhibitors (nonsteroidal antiinflammatory drugs). At the distal end of this cavity lie three residues in close proximity that have been implicated in catalysis by site-directed mutagenesis—Tyr-55, Asp-50, and Lys-84. Tyr-55 is postulated to act as the general acid. 3α-HSD shares significant sequence identity with other HSDs that belong to the aldo-keto reductase superfamily and these may show similar architecture. Other members of this family include prostaglandin F synthase and ρ-crystallin. By contrast, 3α-HSD shares no sequence identity with HSDs that are members of the short-chain alcohol dehydrogenase family but does contain the Tyr-Xaa-Xaa-Xaa-Lys consensus sequence implicated in catalysis in this family. In the 3α-HSD structure these residues are on the periphery of the barrel and are unlikely to participate in catalysis.**

3α-Hydroxysteroid dehydrogenase [3α-HSD; 3α-hydroxysteroid:NAD(P)$^+$ oxidoreductase, EC 1.1.1.50] from rat liver cytosol is a monomeric NAD(P)$^+$-linked oxidoreductase with a molecular mass of 37,029 daltons deduced from its cDNA clone (1). The enzyme reduces biologically important 3-oxo steroids of the androstane (C_{19}), pregnane (C_{21}), and cholane (C_{24}) series, in which the A/B ring fusion may be in the cis or trans configuration (2). These reactions lead to the inactivation of circulating androgens, progestins, and glucocorticoids as well as the biosynthesis of bile acids (3). The enzyme functions as a dihydrodiol dehydrogenase and, by oxidizing *trans*-dihydrodiols of polycyclic aromatic hydrocarbons, can suppress the formation of the ultimate carcinogens: the *anti*-diol epoxides (4). The enzyme also displays 9-, 11-, and 15-hydroxyprostaglandin dehydrogenase activity (5). This multifunctional enzyme is potently inhibited by nonsteroidal antiinflammatory drugs and can be used to screen the antiinflammatory potency of unknowns (6). Structural information is required to understand how this enzyme recognizes its diverse ligands.

The publication costs of this article were defrayed in part by page charge payment. This article must therefore be hereby marked "*advertisement*" in accordance with 18 U.S.C. §1734 solely to indicate this fact.

3α-HSD shares high amino acid sequence identity with bovine lung prostaglandin F synthase (69%), human chlordecone reductase (66%), and frog lens ρ-crystallin (55%), which are members of the aldo-keto reductase superfamily. Included in this family are human placental, bovine, and rat lens aldose reductase, which share 58% sequence identity with 3α-HSD (ref. 1 and references therein). Two newly sequenced HSDs which belong to this family include 20α-HSD from rabbit ovary (7) and bovine testis (8), which share 77% and 58% sequence identity with 3α-HSD, respectively. By contrast, 3α-HSD bears no significant sequence similarity with rat liver 11β-HSD (9), human placental 17β-HSD (10), and 3α,20β-HSD from *Streptomyces hydrogenans* (11), which are members of the short-chain-alcohol dehydrogenase (SCAD) family. This molecular cloning indicates that mammalian HSDs belong to at least two distinct protein families, the aldo-keto reductase superfamily (12) and the SCAD family (13).

Few crystal structures of enzymes that bind steroids are known. These include Δ^5-3-ketosteroid isomerase from *Pseudomonas testosteroni* (14), cholesterol oxidase from *Brevibacterium sterolicum* (15), and 3α,20β-HSD from *Streptomyces hydrogenans* (16). The latter study has been used to draw conclusions about structure–function relationships between members of the SCAD family. This family contains the βαβαβ mononucleotide-binding motif, or Rossmann fold, for NAD(H) binding (17).

We describe the structure of apo 3α-HSD from rat liver to 3.0-Å resolution.¶ It has the architecture of the familiar $(\alpha/\beta)_8$ barrel motif and, in conjunction with sequence alignments, mutagenesis, and affinity-labeling studies, provides information concerning ligand recognition and catalysis.

MATERIALS AND METHODS

Crystallization. Purified 3α-HSD (2) was dialyzed against 10 mM potassium phosphate buffer, pH 7/1 mM EDTA/1 mM 2-mercaptoethanol and concentrated to 12 mg/ml for crystallization. Crystals were grown by vapor diffusion (18) in 6-μl drops of a 1:1 mixture of protein and crystallization buffer [25% (wt/vol) polyethylene glycol 6000/100 mM sodium citrate, pH 5.8/120 mM ammonium sulfate] at 22°C. The crystals grow as flat six-sided plates and belong to the space group $C222_1$ with cell dimensions of a = 51.3 Å, b = 89.5 Å,

Abbreviations: HSD, hydroxysteroid dehydrogenase; ADR, aldose reductase; SCAD, short-chain-alcohol dehydrogenase.

§To whom reprint requests should be addressed.

¶The atomic coordinates have been deposited in the Protein Data Bank, Chemistry Department, Brookhaven National Laboratory, Upton, NY 11973 (reference 1RAL).

and c = 143.3 Å, with one protein monomer per asymmetric unit.

Data Collection. X-ray diffraction data were collected at room temperature on a Siemens multiwire area detector operating at 40 kV and 100 mA. The data were processed using programs written by M.L. A total of 30,872 observations from seven data sets were recorded from four crystals and were reduced to 6122 unique reflections. The reduced data are 96% complete between 10 and 3 Å, with an R_{merge} for all seven data sets of 0.098 [$R_{merge} = \Sigma_{hkl}(\Sigma_i|I - \langle I\rangle|)/(\Sigma_i)$].

Structure Determination. The 3α-HSD structure was solved by the molecular replacement method (19) with the program AMORE (20) using coordinates of human placental aldose reductase (ADR) (21). Data from 10 to 4 Å, and an integration radius of 25 Å, were used for the rotation function (22). The top 10 independent peaks were subjected to a Crowther–Blow translation search (23), and then the top 5 peaks from each translation function (50 total peaks) were refined by rigid-body methods and their packing in the unit cell evaluated. The molecular replacement solution was obvious, with a correlation coefficient between observed and calculated structure factors of 41.1%, an R factor of 43.2%, and sensible packing between symmetry-related molecules within the unit cell.

The structure of 3α-HSD was built in several stages by inspecting $3F_o - 2F_c$ and $F_o - F_c$ difference maps in conjunction with refinement by simulated annealing using XPLOR 3.1 (24). The sequence alignment of 3α-HSD (322 amino acids) and ADR (314 amino acids) (1) was confirmed by examining a difference map made with the preliminary phases of the molecular replacement solution. Based on this alignment, residues unique to the 3α-HSD sequence were built in where the side-chain density was clear, and alanines were placed where only the main-chain density was distinct. In regions where the main-chain density was weak or ambiguous, the residues were omitted from the structure-factor calculation. The electron density at the core of the barrel and the helices was well defined and allowed clear delineation of the side chains with few breaks in the density. However, the density associated with the solvent-exposed loops, especially residues 24–29, was weak. The residues 221–234 as well as the C-terminal residues 309–322 could not be built due to a lack of electron density. A series of $3F_o - 2F_c$ omit maps with 8 residues sequentially omitted helped confirm the model. Typical electron density for a β-sheet region on the side of the barrel is shown in Fig. 1. The R factor from the final cycle of refinement with 3029 protein atoms is 0.220 with an overall B factor of 17.0 Å^2 from 5833 reflections ($F > 1\sigma$) between 10 and 3 Å representing 84% of all possible data. The deviation from ideal geometry for bond lengths and angles was 0.019 Å and 3.8°, respectively.

RESULTS AND DISCUSSION

Molecular Architecture of Rat Liver 3α-HSD. The 3α-HSD structure folds into an α/β, or triose-phosphate isomerase (26), barrel with a cylindrical core of eight parallel β-strands surrounded by eight α-helices which run antiparallel to the β-sheet (Fig. 2). The chain forms the barrel by repeating the β/α unit eight times with two deviations. First, an extra α-helix, H1, exists between β-strand 7 and α-helix 8 (α8), and a second additional α-helix, H2, exists between α8 and the C-terminal region. The secondary structure consists of 33% α-helix and 16% β-sheet.

The bottom of the barrel is sealed by a β hairpin made up of two additional antiparallel β-strands corresponding to residues 6–10 and 13–18 and joined by a tight turn. Solvent-exposed loops, which are only a few residues in length, link the C-terminal ends of the β-strands to the N-terminal ends of the helices, to form the top of the barrel. In addition, there are two large loops that project from the top of the barrel into the solvent: residues 116–142 (loop A), and 217–235 (loop B). The C terminus wanders toward loop A but the electron density becomes disordered after Ala-308. The barrel is essentially elliptical and without the large loops measures about 30 Å × 40 Å × 50 Å. It shows good packing between the hydrophobic residues of the β-strands and α-helices. There are no disulfide bonds despite the existence of nine cysteines.

Cofactor Binding. ADR was the first α/β barrel structure determined that bound NADPH as a cofactor. The structure showed that the pyridine nucleotide does not bind across a Rossmann fold; instead the nucleotide straddles the lip of the barrel. Among the 18 residues involved in binding cofactor to ADR, 12 are conserved in the 3α-HSD sequence. Among these, 8 are positionally conserved, with 6 of these being located in the pocket that would bind the nicotinamide ring and the connected ribose. In addition, it has been shown that 3α-HSD, like ADR, transfers the 4-pro(R) hydrogen from the C-4 position of the nicotinamide ring to the acceptor carbonyl of the substrate (28). Implicit in this observation is that the NADPH should exist in an extended anti conformation. NADPH was modeled into the 3α-HSD structure in the anti conformation by using the coordinates for NADPH in the ADR·NADPH complex. The model of the binary complex shows that the B face of the nicotinamide ring can undergo π stacking with Tyr-216 (Fig. 3). Residues Gln-190, Asn-167, and Ser-166 can all form hydrogen bonds with the carboxamide group of the nicotinamide ring, and conserved residues perform the same function in ADR.

The similarity between the NADPH binding site for 3α-HSD and ADR, however, ends in the region that binds the pyrophosphate bridge and may be related to several factors. A conformational change has been shown to occur upon

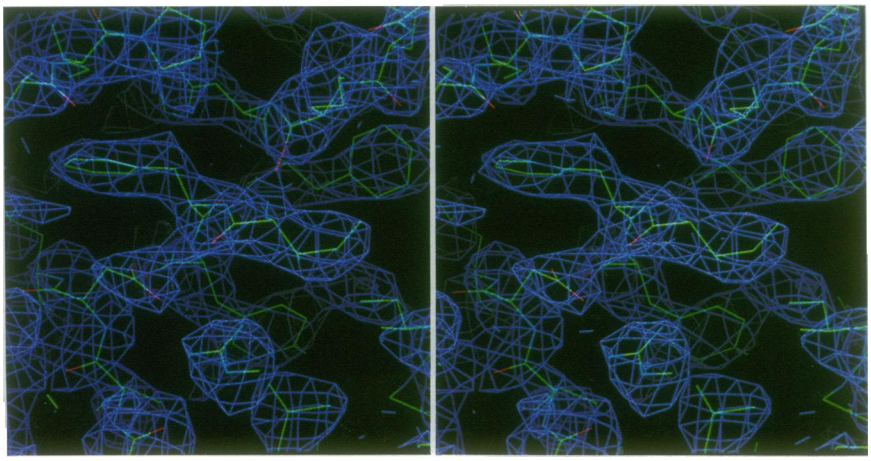

FIG. 1. Stereoview of representative electron density showing β-strands 3 and 4, using the molecular graphics program CHAIN (25). The map was calculated at 3-Å resolution with $3F_o - 2F_c$ amplitudes and model phases, contoured at 1 standard deviation.

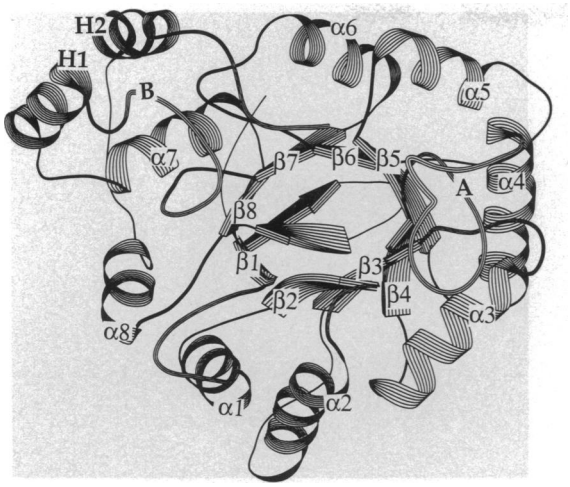

FIG. 2. A RIBBON plot (27) viewed down the barrel axis with the C terminus at the top. The secondary structure elements and loops are labeled. Loop B and the C terminus following Ala-308 are disordered.

binding the cofactor to human ADR (21, 29) which involves residues of the N-terminal region of loop B. The structure of the ADR complex revealed a novel NADPH binding motif which has been described as a "safety belt," in which the pyrophosphate is locked into position by lying in a tunnel lined with residues which could hydrogen bond to the phosphate oxygens. The N-terminal portion of the loop is locked into place by two salt links. In 3α-HSD, this loop (loop B) is disordered from residue 221 to residue 234, probably because of the high mobility of this region and a lack of a cofactor to stabilize it. Further, 3α-HSD catalyzes an ordered bi–bi mechanism, and the association of the first ligand, NAD(P)(H), is rate limiting (28), indicating that a conformational change also occurs on binding cofactor. Conformational changes involving the loops of α/β-barrel enzymes have been previously associated with ligand binding (30).

3α-HSD binds both NADH and NADPH. In examining the specificity of flavoprotein disulfide oxidoreductases for pyridine nucleotides, it was found that in addition to containing a Rossmann fold, those proteins which preferred NADPH contained two highly conserved arginines 6 residues apart (31). These two charged residues specifically interacted with the negatively charged oxygens on the phosphate of 2′-AMP. Lys-262 and Arg-268 in the ADR structure provide the same interactions with the 2′ phosphate of AMP. The equivalent residues in the 3α-HSD sequence are Arg-270 and Arg-276 and may contribute to the higher affinity of 3α-HSD for NADPH. The K_d for NADPH is 195 nM and that for NADH is 158 μM (32).

The only other HSD whose atomic structure is known, 3α,20β-HSD from *Streptomyces hydrogenans*, has the canonical Rossmann fold for binding pyridine nucleotide. This enzyme binds NAD(H) in an extended syn conformation, consistent with the transfer of the 4-pro(*S*) hydrogen, and is a member of the SCAD family (16). The other HSDs that belong to this family (11β-HSD and 17β-HSD) may also possess the Rossmann fold. By contrast, our study predicts that HSDs that belong to the aldo-keto reductase superfamily do not bind cofactor in this manner.

Catalytic Triad. Based on the proximity that must exist between the C-4 position of the nicotinamide ring and the acceptor carbonyl on the substrate, a catalytic triad was identified in the crystal structure of ADR as Tyr-48, Lys-77, and Asp-43. Having shown that the nicotinamide ring of NAD(P)H could bind in an identical fashion in the 3α-HSD model, we found a similar triad conserved in sequence and location in our model as Tyr-55, Lys-84, and Asp-50. Thus a mechanism can be proposed for the oxidoreduction catalyzed by 3α-HSD (Fig. 4). In this mechanism, hydride transfer to the ketone at the C-3 position of the steroid would be facilitated by a proton relay. During reduction, Tyr-55 would act as a general acid by donating the proton of the phenolic hydroxyl group to the steroid carbonyl. The pK_a of the tyrosine may be lowered to the pH optimum of the enzyme by forming a hydrogen bond to Lys-84, which in turn is stabilized by a salt link to Asp-50. A tyrosine residue, despite its high pK_a in water, has been implicated as the general acid in the reaction mechanism of Δ^5-3-ketosteroid isomerase (33). This catalytic triad is conserved in all published ADR sequences. In the 3α-HSD model, the triad is located at the bottom of a hydrophobic cavity, at the C-terminal ends of β-strands 2 and 3. When NADPH is modeled into the 3α-HSD structure, the B face of the nicotinamide ring stacks against Tyr-216 and exposes the A face to the active site, allowing transfer of the 4-pro(*R*) hydrogen to the β face of the steroid. Site-directed mutagenesis studies confirm the importance of the triad (42). Substitution of phenylalanine for Tyr-55 produced a mutant enzyme (Tyr55Phe) which was inactive but still formed binary (E·NADPH) and ternary complexes (E·NADH·testosterone). In this mutant the affinity for cofactor was unaltered, suggesting that a global conformational change had not occurred. By contrast the affinity of the E·NADH complex for testosterone was reduced by a factor of 30, implicating this residue in both catalysis and steroid binding. Our model would predict that Tyr-55 performs both these functions since it is located at the bottom of the hydrophobic cavity. Additionally, the mutant enzymes Asp50Asn and Lys84Arg have been shown to be catalytically inactive (T.M.P. and B. Schlegel, unpublished data). Although His-117 is also close to the nicotinamide ring and may be involved in the proton relay, its local hydrophobic environment (Phe-118 and Trp-86) may lower the pK_a of the residue to below the pH optimum for catalysis.

The Hydrophobic Cavity and Steroid Hormone Recognition. A large hydrophobic cavity resides near the top of the barrel and is located on the loops at the C ends of the β-strands (Fig. 5). Hydrophobic amino acids abound in this cavity: Leu-54, Tyr-55, Trp-86, Phe-118, Phe-129, and Tyr-216 are conserved with respect to ADR and show similarity in sequence align-

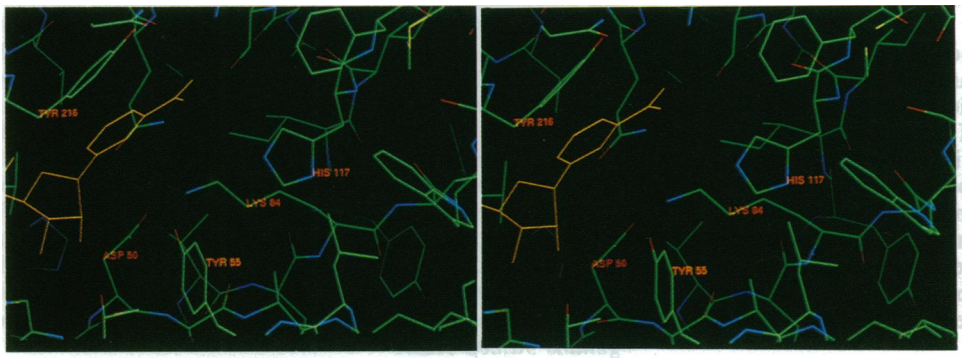

FIG. 3. Stereoview showing the nicotinamide ring modeled into the active site within π stacking distance of Tyr-216. The proposed catalytic triad—Tyr-55, Lys-84, and Asp-50—is shown. Tyr-55 is close enough to Lys-84 to form the proposed hydrogen bond. His-117 is also shown in its local hydrophobic environment.

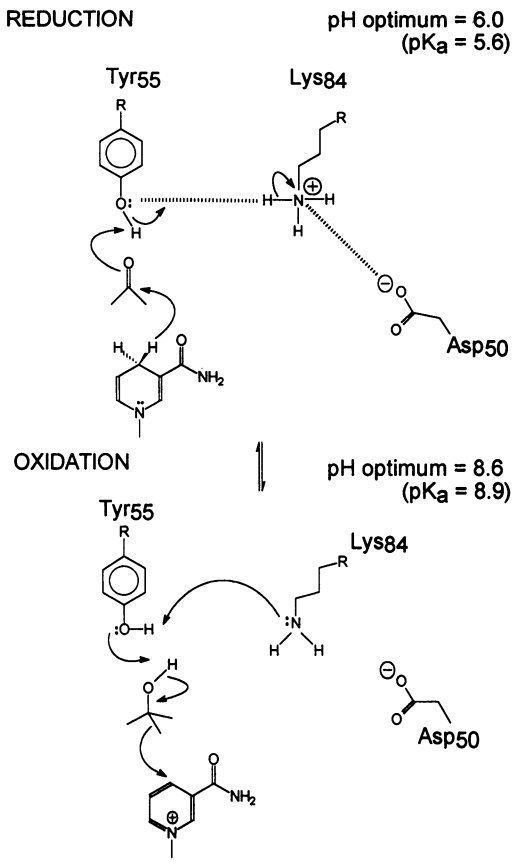

FIG. 4. Proposed mechanism of catalysis for 3α-HSD. pK_a values determined from pH rate profiles are 5.6 for reduction and 8.9 for oxidation.

ment to other HSDs that are members of the aldo-keto reductase superfamily (bovine testis 20α-HSD and rabbit ovary 20α-HSD). These residues are implicated in binding hydrophobic substrates (steroids, prostaglandins, and polycyclic aromatic hydrocarbons) and inhibitors (nonsteroidal antiinflammatory drugs). The hydrophobic cavity is about 11 Å deep, projects toward the center of the barrel, and could easily accommodate steroid hormones. The distance from O(C-3) to O(C-17) on 5α-androstane-3,17-dione is 10.8 Å. The catalytic triad is at the distal end of the hydrophobic pocket.

In the ADR structure another tryptophan is implicated in binding hydrophobic substrates. The corresponding residue in 3α-HSD is Trp-227 and is included in the presumptive steroid binding site even though it is found in loop B, which is disordered in the structure. Two other phenylalanine residues are included in the hydrophobic pocket in ADR, the equivalent residues in 3α-HSD being Phe-128 and Phe-129. These residues are not conserved in rabbit ovary 20α-HSD, prostaglandin F synthase, or chlordecone reductase, and this may reflect differences in substrate specificity among these highly similar proteins.

The C terminus of ADR has been implicated in substrate binding (34). A mutant with the last 13 residues deleted had greatly decreased catalytic efficiency for uncharged substrates, while the K_m for NADPH was unaltered. This indicates that the C terminus of ADR is not involved in cofactor binding but is critical to the proper orientation of the substrate. 3α-HSD shares 40% sequence similarity with ADR in this region, but in the present structure the C terminus is disordered. These residues may become more ordered upon binding of steroid. Crystallographic studies of a ternary (E·NADPH·steroid) complex are required to better define the topography of this site.

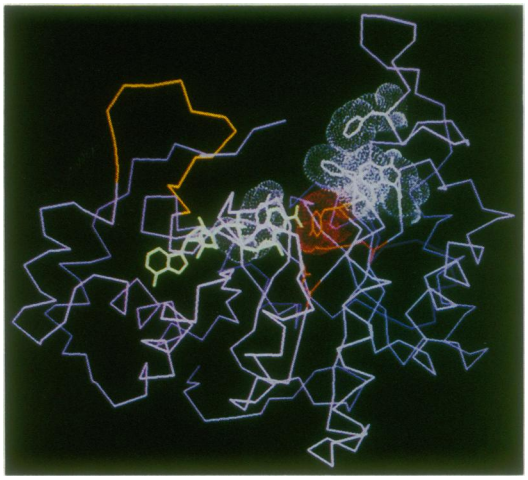

FIG. 5. C^{α} trace of the side view of the barrel with large loops projecting from the C-terminal end of the barrel. The orientation is about 90° from that of Fig. 2. NADPH (in yellow) modeled into the structure lies across the top of the barrel. The disordered loop B is shown in orange. Dot surfaces showing 100% of van der Waals radii cover the residues in the hydrophobic cavity (in pink) and the proposed catalytic triad (in red). The C terminus is shown only up to Ala-308, with the remaining residues disordered.

Affinity-labeling studies of 3α-HSD using bromoacetoxysteroids have implied that Cys-170, Cys-242, and Cys-217 are points of contact with C-3, C-11, and C-17 of the steroid nucleus (35). However, our model shows that Cys-170 and Cys-242 are located on the periphery of the barrel on α-helix 5 and α-helix H2, respectively, and that they are not associated with the hydrophobic pocket implicated in steroid binding (Fig. 6). Only Cys-217, directly above β-strand 7, is located toward the C-terminal lip of the barrel. In α/β-barrel enzymes, active-site residues are usually located in the loops which connect a β-strand with the following α-helix, and are always in the C-terminal half of the barrel (36).

Site-directed mutagenesis studies where these cysteines were mutated to alanines can now be rationalized (42). Cys170Ala and Cys242Ala mutants were kinetically similar to wild-type recombinant 3α-HSD. The 3α-HSD structure supports the concept that Cys-170 and Cys-242 are most likely modified by bromoacetoxysteroids, since of the nine cysteines, they are the most accessible and have local hydrophobic environments. However, the Cys217Ala mutant demonstrated a 4-fold increase in the K_m for 5α-androstane-3,17-dione and a 2-fold increase in the K_m for NADH. Although Cys-217 is not formally part of the hydrophobic cavity, it is nearby. Moreover, the equivalent residue in ADR, Ser-210, is involved in hydrogen bonding to the pyrophosphate of NADPH (21). Cys-217 may be involved in either steroid and/or cofactor binding, since it is at the interface of both sites.

SCAD Consensus Sequence. 3α-HSD is representative of the mammalian HSDs that belong to the aldo-keto reductase superfamily and shares no significant sequence identity with HSDs that have been assigned to the SCAD family (13). Other members of the SCAD family include 15-hydroxyprostaglandin dehydrogenase (37) and *Drosophila* alcohol dehydrogenase (38). Members of the SCAD family share the consensus sequence Tyr-Xaa-Xaa-Xaa-Lys, which is strictly conserved. Mutagenesis studies on these enzymes have implicated this tyrosine in catalysis (39–41). For *Drosophila* alcohol dehydrogenase, it was inferred that this tyrosine was the general acid and that the lysine lowered its effective pK_a (41). Both these residues are located at the presumed steroid binding site in the crystal structure of *Streptomyces hydrogenans* 3α,20β-HSD.

FIG. 6. A cartoon of the structure looking down the barrel connecting only the α carbons, in the same orientation as Fig. 2. The modeled NADPH lying across the lip of the barrel is shown in ball-and-stick form. Cys-242 and Cys-170, on α-helices H1 and α5, respectively, and Cys-217 are shown in yellow. The residues forming the hydrophobic cavity are shown in pink. Residues of the proposed catalytic triad, Tyr-55, Lys-84, and Asp-50, are shown in red. The consensus SCAD sequence is in blue showing the positions of Tyr-205 and Lys-209. The disordered loop B is shown in orange. The C terminus is shown up to Ala-308.

3α-HSD shares this consensus sequence at residues 205–209, as Tyr-Cys-Lys-Ser-Lys. These residues in 3α-HSD are on α-helix 6, on the periphery of the molecule facing the solvent (Fig. 6). Analysis of the 3α-HSD Tyr205Phe mutant indicated that this was kinetically unaltered from wild type, supporting the noninvolvement of this tyrosine in 3α-HSD catalysis (42). It is intriguing that HSDs in the aldo-keto reductase family and the SCAD family may both use similar catalytic mechanisms but the tyrosine and lysine residues involved are different. Hydride transfer using tyrosine as the general acid may be a common theme in all HSD catalysis.

We thank Dr. Florante Quiocho and David Wilson of the Howard Hughes Medical Institute and Department of Biochemistry at Baylor College of Medicine for the coordinates of aldose reductase. We thank Dr. Phil Jeffrey for his very helpful advice in the refinement of the structure. This research was funded by Department of Defense Grant DAAL03-92-G-0173 and National Institutes of Health Grants GM44617, DK47015, and CA39504. S.S.H. was a recipient of a Biophysical Spectroscopy Training Fellowship (S-T32-GM08275). T.M.P. is a recipient of a Research Career Development Award from the National Cancer Institute (CA01335).

1. Pawlowski, J. E., Huizinga, M. & Penning, T. M. (1991) *J. Biol. Chem.* **266**, 8820–8825.
2. Penning, T. M., Mukharji, I., Barrows, S. & Talalay, P. (1984) *Biochem. J.* **222**, 601–611.
3. Takikawa, H., Ookhtens, M., Stolz, A. & Kaplowitz, N. (1987) *J. Clin. Invest.* **80**, 861–866.
4. Smithgall, T. E., Harvey, R. G. & Penning, T. M. (1986) *J. Biol. Chem.* **261**, 6184–6191.
5. Penning, T. M. & Sharp, R. B. (1987) *Biochem. Biophys. Res. Commun.* **148**, 646–652.
6. Penning, T. M. & Talalay, P. (1983) *Proc. Natl. Acad. Sci. USA* **80**, 4504–4508.
7. Lacy, W. R., Washenick, K. J., Cook, R. G. & Dunbar, B. S. (1993) *Mol. Endocrinol.* **7**, 58–66.
8. Warren, J. C., Murdock, G. L., Ma, Y., Goodman, S. R. & Zimmer, W. E. (1993) *Biochemistry* **32**, 1401–1406.
9. Agarwal, A. K., Monder, C., Eckstein, B. & White, P. C. (1989) *J. Biol. Chem.* **264**, 18939–18943.
10. The, V. L., Labrie, C., Zhao, H. F., Couët, J., Lachance, Y., Simard, J., Lablanc, G., Côté, J., Bérubé, D., Gagné, R. & Labrie, F. (1989) *Mol. Endocrinol.* **3**, 1301–1309.
11. Marekov, L., Krook, M. & Jörnvall, H. (1990) *Fed. Eur. Biochem. Soc.* **266**, 51–54.
12. Bohren, K. M., Bullock, B., Wermuth, B. & Gabbay, K. H. (1989) *J. Biol. Chem.* **264**, 9547–9551.
13. Krozowski, Z. (1992) *Mol. Cell. Endocrinol.* **84**, C25–C31.
14. Westbrook, E. M., Piro, O. E. & Sigler, P. B. (1984) *J. Biol. Chem.* **259**, 9096–9103.
15. Vrielink, A., Lloyd, L. F. & Blow, D. M. (1991) *J. Mol. Biol.* **219**, 533–554.
16. Ghosh, D., Weeks, C. M., Grochulski, P., Duax, W. L., Erman, M., Rimsay, R. L. & Orr, J. C. (1991) *Proc. Natl. Acad. Sci. USA* **88**, 10064–10068.
17. Rossmann, M. G., Liljas, A., Brändén, C. I. & Banaszak, L. J. (1975) in *The Enzymes*, ed. Boyer, P. D. (Academic, New York), Vol. 11A, pp. 61–102.
18. McPherson, A. (1989) *Preparation and Analysis of Protein Crystals* (Krieger, Malabar, FL), p. 96.
19. Rossmann, M. G. & Blow, D. M. (1962) *Acta Crystallogr.* **15**, 24–31.
20. Navaza, J. (1992) in *Proceedings of Daresbury Study Weekend on Molecular Replacement*, eds. Dodson, E. J., Gover, S. & Wolf, W. (SERC Daresbury Laboratory, Warrington, U.K.), pp. 87–90.
21. Wilson, D. K., Bohren, K. M., Gabbay, K. H. & Quiocho, F. A. (1992) *Science* **257**, 81–84.
22. Navaza, J. (1987) *Acta Crystallogr. A* **43**, 645–653.
23. Crowther, R. A. & Blow, D. M. (1967) *Acta Crystallogr.* **23**, 544–548.
24. Brünger, A. T., Kuriyan, J. & Karplus, M. (1987) *Science* **235**, 458–460.
25. Sack, J. S. (1988) *J. Mol. Graphics* **6**, 224–225.
26. Banner, D. W., Bloomer, A. C., Petsko, G. A., Phillips, D. C., Pogson, C. I., Wilson, I. A., Corran, P. H., Firth, A. J., Milman, J. D., Offord, R. E., Priddle, J. D. & Waley, S. G. (1975) *Nature (London)* **255**, 609–614.
27. Priestle, J. (1988) *J. Appl. Crystallogr.* **21**, 572–576.
28. Askonas, L. J., Ricigliano, J. W. & Penning, T. M. (1991) *Biochem. J.* **278**, 835–841.
29. Borhani, D. W., Harter, T. M. & Petrash, J. M. (1992) *J. Biol. Chem.* **267**, 24841–24847.
30. Joseph, D., Petsko, G. A. & Karplus, M. (1990) *Science* **249**, 1425–1428.
31. Scrutton, N. S., Berry, A. & Perham, R. N. (1990) *Nature (London)* **343**, 38–43.
32. Ricigliano, J. W. & Penning, T. M. (1990) *Biochem. J.* **269**, 749–755.
33. Li, Y.-K., Kuliopulos, A., Mildvan, A. S. & Talalay, P. (1993) *Biochemistry* **32**, 1816–1824.
34. Bohren, K. M., Grimshaw, C. E. & Gabbay, K. H. (1992) *J. Biol. Chem.* **267**, 20965–20970.
35. Penning, T. M., Abrams, W. R. & Pawlowski, J. E. (1991) *J. Biol. Chem.* **266**, 8826–8834.
36. Farber, G. K. & Petsko, G. A. (1990) *Trends Biochem. Sci.* **15**, 228–234.
37. Krook, M., Marekov, L. & Jörnvall, H. (1990) *Biochemistry* **29**, 738–743.
38. Thatcher, D. R. (1980) *Biochem. J.* **187**, 875–886.
39. Ensor, C. M. & Tai, H.-H. (1991) *Biochem. Biophys. Res. Commun.* **176**, 840–845.
40. Obeid, J. & White, P. C. (1992) *Biochem. Biophys. Res. Commun.* **188**, 222–227.
41. Chen, Z., Jiang, J. C., Lin, Z.-G., Lee, W. R., Baker, M. E. & Chang, S. H. (1993) *Biochemistry* **32**, 3342–3346.
42. Paulowski, J. E. & Penning, T. M. (1994) *J. Biol. Chem.*, in press.